Monte-Carlo Model for Describing Charge Transfer in Irradiated CCDs

Dennis Gallagher , Raymond Demara,
Gary Emerson, Wayne Frame, and Alan Delamere

Ball Aerospace and Technologies Corp.
Boulder, Colorado 80306

Abstract

Radiation exposure of CCD devices degrades the charge transfer inefficiency (CTI) by the creation of electron trap sights within the bulk silicon. The presence of electron traps tend to smear the signal of a point-like image. This affects CCDs used in star trackers where sub-pixel centroiding is required for accurate pointing knowledge. To explore the effects of radiation damage in CCD devices, we have developed a Monte-Carlo model for simulating charge transfer in buried channel CCDs. The model is based on the Shockley-Read-Hall generation-recombination theory. The CTI in CCD devices was measured before and after exposure to mono-energetic 61 MeV protons. Our data show that displacement damage in the bulk silicon increases the CTI of the CCD device. CTI was measured on irradiated CCD devices at various temperatures from -10 to -150 Celsius, thus providing estimates of the electron trap energy levels created in the CCD silicon. The dominate post-radiation trap energy level was the silicon E-center found to be at an energy of 0.46 eV, which is in good agreement with other published values. To fit our data over the complete temperature range, we also required electron traps of 0.36 eV and 0.21 eV. Our model also includes the effects of charge cloud growth with signal volume and clocking rates of the CCD device. Determining the types and levels of radiation a CCD device will encounter during its operational life is very important for choosing CCD operating parameters.

1.0 Introduction

Defect sites in the bulk silicon of a CCD are created when it is placed in a high charge particle radiation environment. The increase in charge transfer inefficiency (CTI) after exposure to radiation affects the radiometric calibration of the CCD and also creates smearing for point-like images. The latter has adverse effects in CCDs used for star tracker and astronomical applications. Prior to radiation damage the parallel CTI of a 512X512 device is normally very small, on order 10^{-6} , but after significant exposure to space radiation or a simulated space environment through the use of high energy proton fluences, we have seen the CTI increase to on order 10^{-3} . Even with significant shielding of a flight CCD device with several centimeters of aluminum, the CTI will still increase from radiation damage during the life of a multi-year mission. In this paper we discuss results of radiation testing on SITE 502AF 512X512 front illuminated CCD devices. We have developed a model that describes the post-radiation damaged CTI dependence on temperature. Finally, we use the CTI model in a Monte Carlo simulation program that simulates the transfer of an image from a CCD. Results from simulation agree well with data collected during illumination of a CCD by a Fe^{55} source. This model will be used to predict centroiding errors for CCDs used in star tracker applications as a function of their time in the space radiation environment.

2.0 Charge Transfer Inefficiency Model

Since the trap sites are caused by defects introduced into the silicon lattice structure, the traps tend to occur with specific energy levels. The Shockley Read Hall theory (SRH), as originally applied to CCDs by (Mohsen and Thompsett , 1974), describes how the traps capture and emit electrons. The theory parameterizes the traps using electron emission and capture time constants. The emission and capture time constants are temperature dependent due to the kT nature of the trap energy levels. If the thermal energy of the silicon is much above the kT energy of a trap, then the trap will capture and emit electrons very quickly and the trap will have little effect on the CTI as a charge packet is transferred through a pixel. As the thermal energy

SPIE Vol. 3301 • 0277-786X/98/$10.00

approaches the trap energy, the traps will tend to remove electrons from a transferring charge packet and reemit them later thus increasing the CTI . When the thermal energy is well below the trap energy, the trap will tend to stay filled, by dark current electrons, during the CCD read time and no charge will be removed by the traps during charge transfer reducing the CTI. Dark current has a strong influence on the CTI at thermal energies above the kT trap energy because traps are filled by dark current electrons creating a "fat zero" effect and decreasing the CTI. For typical CCD operating conditions the capture time constant is typically much less than 1 μs, and the emission time constant on order several seconds to a milli-second. For CCDs with read out clock rates less than 1 MHz, the capture time of the traps can be assumed to be instantaneous, that is, if there are traps in a pixel they will be filled by any charge that passes through the pixel up to the available charge in the signal. The emission time constant is described by equation (1)

$$\tau_e = \frac{g}{\sigma_n v_t N_c} \exp\left(\frac{E_t}{kT}\right) ; \quad v_t N_c = 1.6\times 10^{21} \bullet T^2 s^{-1} cm^{-2} \tag{1}$$

where g~0.5 accounts for the degeneracy of the level, σ_n is the temperature independent cross-section for the trap (cm^2), v_t is the thermal velocity ($cm\ sec^{-1}$), N_c is the conduction band density of states, E_t is the energy level of the trap in eV, and k represents Bolzmann's constant and T the temperature. For a typical CCD, the per pixel parallel transfer takes longer than the per pixel serial transfer and hence parallel transfer (parallel CTI) is more affected by radiation damage. During parallel transfer empty pixels will have a greater time to emit electrons, thus leaving traps that will remove electrons from the signal when it is clocked through the pixels with empty traps. Another factor is that all signal passes through the serial register which will tend to keep traps in the serial registers filled reducing serial CTI. The time duration between signal charge packets (Fe^{55} hits) affects the CTI where the greater their density, the lower the CTI due to the "fat zero" effect. Also, the level of the signal in a pixel will affect CTI where large signal levels will have more available electrons to fill traps reducing the CTI. The CTI for a single pixel transfer can be described by a simplified version of the SHR equation given by equation (2) from (Dale et al. 1993) .

$$CTI = \left(\frac{V_s}{N_s} \bullet N_t\right)\left(\exp\left(-\frac{T_t}{\tau_e}\right)\right)\left(1-\exp\left(-\frac{T_s}{\tau_e}\right)\right) \tag{2}$$

Where N_t is the trap density in cm^{-3}, V_s is the volume occupied by the charge in cm^3, N_s is the number of electrons in the signal, T_t is the per pixel clocking time of the CCD, and T_s is the time between signal packets given by equation (3).

$$T_s = NX \bullet T_t + NX \bullet T_t * N_{serial} \tag{3}$$

where NX is the number of 'empty' pixels between pixels with signal, and N_{serial} is the number of serial transfers, including any extended and over-clocking in the serial direction. If different energy level traps are present, then their terms (using their respective emission time constants) are added to equation (2) in the following manner,

$$CTI = \left(\frac{V_s}{N_s} \bullet N_t\right) \times \left[\left(\exp\left(-\frac{T_t}{\tau_{e_1}}\right)\right)\left(1-\exp\left(-\frac{T_s}{\tau_{e_1}}\right)\right) + \left(\exp\left(-\frac{T_t}{\tau_{e_2}}\right)\right)\left(1-\exp\left(-\frac{T_s}{\tau_{e_2}}\right)\right) + \ldots\ldots\right] \tag{4}$$

Equation (4) describes the effects that certain trap energies will dominate the CTI over other traps depending on their temperature dependent emission time constants.

To include the effects of dark current an additional term has been added to equation (4) to account for the filling of traps by non signal dark current electrons, which will tend to improve the high temperature CTI (Holland, 1993). Equation (5) shows the correction for dark current electrons

$$\mathrm{CTI} = \mathrm{equation}(4) \times \frac{N_s}{N_s + D \bullet T_{\text{read time}}} \tag{5}$$

Where D is the dark current generation in $\left(\text{electrons pixel}^{-1}\,\text{sec}^{-1}\right)$ and $T_{\text{read time}}$ (sec) is the total time required to read the CCD image.

3.0 The Experiment

Figure 1 shows one of the test chambers in the Center for Solid State Imaging (CSSI) labs at Ball Aerospace. The test chamber is pumped by sorbitive getter pumps using liquid nitrogen to freeze out the air to about 10-30 mill-torr. The test system is fully automated, with exposure times, Fe^{55} source location, and temperature all under computer control . The CCD temperature is maintained to within 0.1 Celsius of the desired operating temperature by a closed loop temperature controller using both heater power and liquid nitrogen. The temperature was varied from -10 to -150 Celsius.

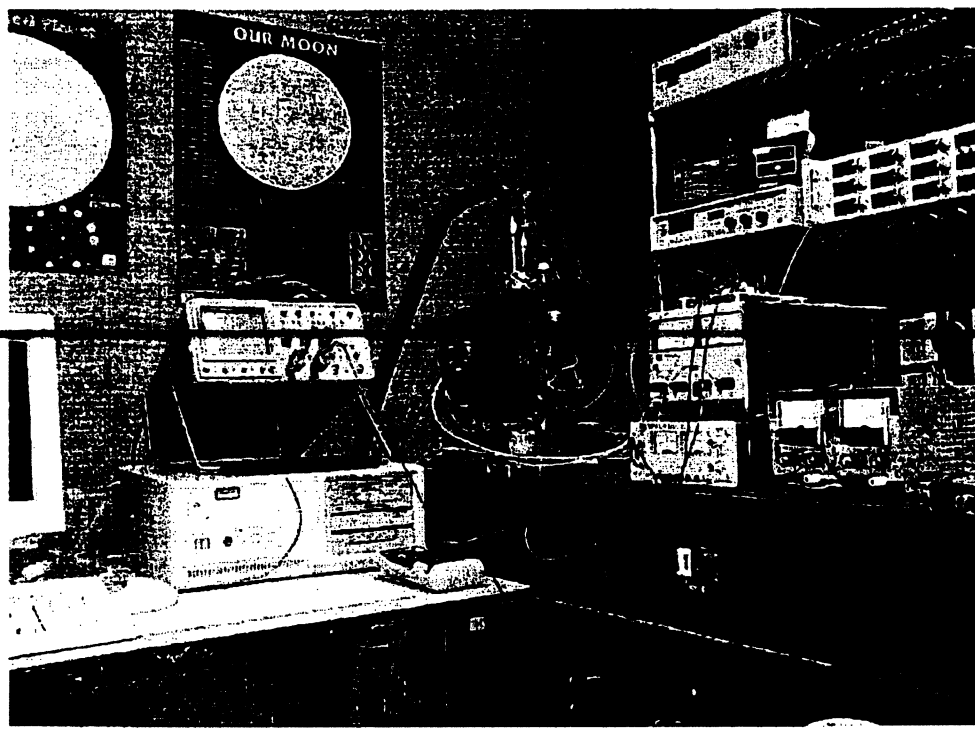

Figure 1: The CCD test facility at Ball Aerospace used for conducting research with CCDs. The dark cylindrical object is one of the 250 mm diameter vacuum test chambers. The electronics to the right are used for setting the clocking and rail voltages of the CCD along with a correlated double sampler for reading the CCD used in these tests

The CCDs we evaluated were front illuminated SITE SI-502AF 512X512 24 micron pixel devices. Charge packets of ~1620 electrons were created in the CCD by illuminating the CCD with an Fe^{55} source. Hit densities were about one Mn-K(α,β) photon every 50 pixels. The entire CCD was read through one of the two on-chip amplifiers. After pre-radiation CTI evaluation, six of the seven CCDs were irradiated with 61 MeV protons at the Crocker Nuclear Laboratory at the University of California, Davis CA. Three fluence levels were used, with two CCDs tested at each fluence level. The fluence levels were 5.4×10^{10} protons cm^{-2}, 2.7×10^{10} protons cm^{-2}, and 1.4×10^{10} protons cm^{-2}. A total fluence of 2.7×10^{10} protons cm^{-2} at 61 MeV represents the predicted end-of-life proton exposure behind 25 mm of aluminum shielding for an 833 km, 98.7° inclined, orbit after 7 years in space. The CTI was then measured again for each device. Figure 2 shows the measured CTI values as a function of temperature. One CCD had the CTI evaluated down to -150 C to measure the effect of the low energy traps on the CTI. The increase in CTI below about -110 C clearly indicates the presence of a low energy trap. No pre-radiation data were collected below -80 C

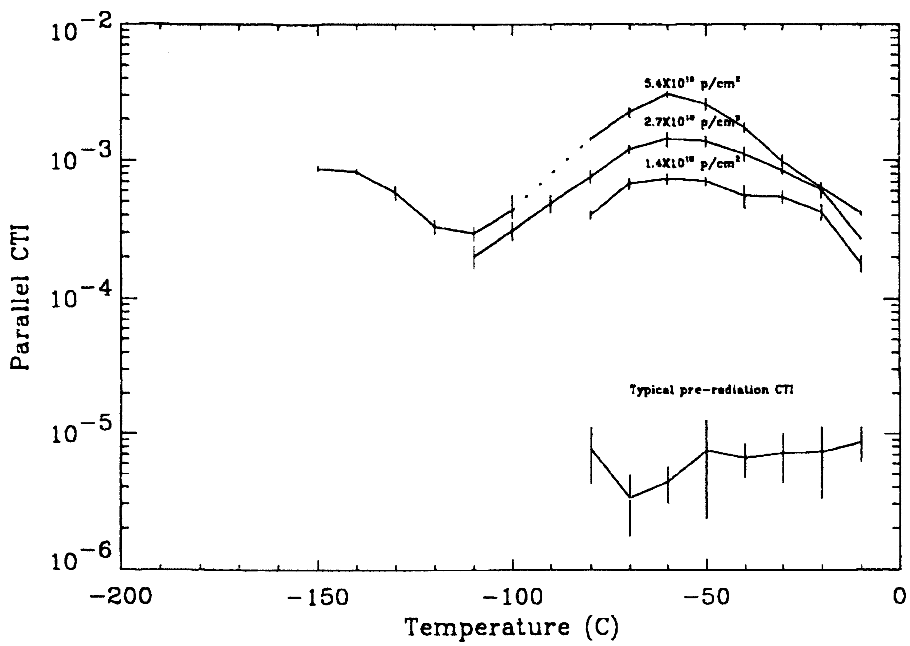

Figure 2: Measured Post-radiation CTI as function of temperature . The CTI was calculated by adding two images with Fe^{55} hits. The average CTI measured for five pairs of images is shown . The error bars are $\pm 1\sigma$ which were determined from the standard deviation in the five CTI values obtained at each temperature.

4.0 Radiation Induced Traps

Traps in irradiated CCDs have been found to occur at certain energies with some spread in their reported values (C. Dale et al. 1993,A. Holland 1993). A good example of trap energies and their cross sections found in irradiated CCDs is given by Holland (1993) which are reproduced in Table I. The number density N_t of the traps given in Table I are for CCDs irradiated with 10 MeV protons at $3.6 X 10^9$ protons cm^{-2}. The trap level at $E_c - E = 0.42$ eV has been reported in the literature to be at energies in the range of 0.40-0.46 eV and is only seen in CCDs that have been exposed to high energy particles. We applied the above CTI model given by equations 4 and 5 to our data.

Table I Trap Energies found in irradiated CCDs, cross sections, and number densities

Trap Name	$E_c - E$ (eV)	cross section (cm^2)	N_t (cm^{-3})
Trap A	0.12	1×10^{-14}	6×10^{10}
Trap B	0.30	1×10^{-14}	7×10^{9}
Trap C	0.42	6×10^{-15}	3×10^{10}

To apply the dark current correction to the CTI model, (*D* in equation 5), each CCD device had its post radiation dark current measured as a function of temperature. The dark current temperature profiles were then fitted to derive an empirical equation for dark current for each radiation fluence level. Only one dark current equation was derived for each pair of CCDs because radiation fluence levels dominated what the dark current would be rather than device dependent parameters after irradiation. Table II gives the equations for each of the dark current fits.

Table II Equations describing dark current at each fluence level

1.4×10^{10} protons cm^{-2}	$1800\times EXP(T/8.8)$ e^- / pixel / sec
2.7×10^{10} protons cm^{-2}	$2500\times EXP(T/9.0)$ e^- / pixel / sec
5.4×10^{10} protons cm^{-2}	$3100\times EXP(T/10.6)$ e^- / pixel / sec

CCD CTI Test Parameters used in model

The following parameters of the test setup were used as input to the CTI model given by (Equations 4 and 5). To fit the model to the data, the trap energy and the site defect number density were allowed to change. Figure 3 shows the data and the fits with the model.

SITE SI-502AF 512X512 CCD Test Configuration

Pixel size 24X24 μm pixels	$V_s = 24\times6\times0.15\times(1\times10^{-12})$ cm^3
Serial clock rate 41.6 kHz/pixel	$T_t = 24\times10^{-6}$ sec
Parallel clock rate 13.3 milli-sec/pixel	$= T_t * N_{serial}$
Signal is Fe 55 or 1620 electrons	$N_s = 1620e^-$
Signal density ~ 1 X-ray/ 50 pixels	NX=50
Dark current	D=equation(5) ,TableII electrons $pixel^{-1}sec^{-1}$
CCD read time	$T_{read\ time}$ =7.3 sec
Trap cross sections	from Table I τ_e sec
Conduction band density thermal velocity	$v_t N_c$, Equation(1)

**The 6 μm dimension is due to the size of CCD mini channel. The 0.15 μm is a typical height of signal charge cloud size (Holland, 1993.).*

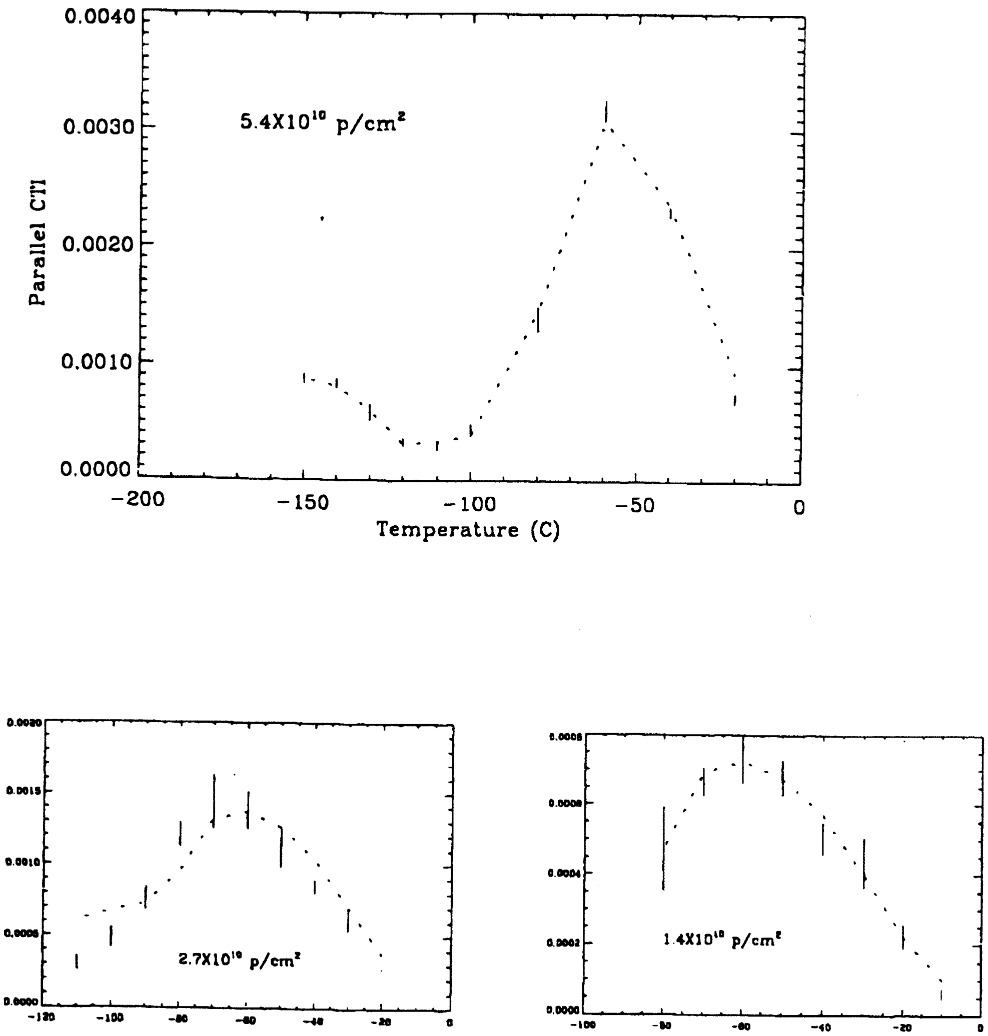

Figure 3: Results of the CTI model (dashed line) using (Equations 4 and 5) and measured CTI data.. The error bars represent the 1σ uncertainties.

A χ^2 analysis was performed with the model and data for the most irradiated CCD, which was also tested to the coldest temperatures (upper plot in figure 3). The trap cross sections were taken from table I where the highest trap energy was assigned the highest energy cross section in Table I and so forth. The variables that were adjusted to fit the data were the trap energies and trap number densities N_t. Only the data for the most irradiated chip was used for the trap energy analysis. Table III shows the trap energies giving the minimum χ^2 ($\Sigma\chi^2 = 28$). The lower plots in figure 3 show the data and model for the CCDs irradiated at the lower fluences. The fit to these curves were derived using the trap energies in table III and the Interactive Data Language "curvefit" routine to fit the trap number density. The lowest trap energy was not used to fit these curves due to no data being taken below -110 C for the CCDs irradiated at the lower fluences. The uncertainties for trap energy are quoted as 1σ; a $\Delta\chi^2$ ~3 for the 3 parameter (energy) fit.

Table III Post-Radiation trap energies, and number densities derived from data

	Nt (cm^{-3})		
$E_c - E$ (eV)	1.5×10^{10} p / cm^{-2}	1.7×10^{10} p / cm^{-2}	5.4×10^{10} p / cm^{-2}
0.458 ± 0.006	3.6×10^{10}	6.0×10^{10}	2.3×10^{11}
0.358 ± 0.016	2.3×10^{10}	5.0×10^{10} ?	2.2×10^{10}
0.213 ± 0.004	NA	NA	7.4×10^{10}

The two highest trap energies required to fit the data agree well with values that were obtained by deep level transient spectroscopy (Watts, 1996). The trap number densities are somewhat difficult to compare with others because of the CCD device dependent parameters and various radiation exposure conditions. The number density for the 0.36 eV trap for the CCD irradiated to 1.7×10^{10} p / cm^{-2} is in question. Because of the exponential dependence of CTI on trap energy level, the fit to the data has a strong dependence on trap energy. The low energy trap level at 0.21 eV is close to the 0.17, 0.18 eV traps reported by (Holland, Dale), but we were unable to fit the low temperature region of the CTI curve using these energy levels .

5.0 Monte-Carlo Simulation

A Monte-Carlo model was written to simulate the effects of CTI on charge transfer in the reading of a CCD image. We choose to model the Fe^{55} images we collected during the CTI measurements. The simulation uses the CTI values as determined by Equation 5. The input parameters to the model are shown in the CCD Test Configuration shown previously. The transfer of an electron by the model is performed using a uniform random number between 0-1 which is compared to the calculated CTI for a given pixel. If the random number is greater than the CTI the electron is transferred to the next pixel. Dark current is also included in the model also through a randomized process. Figure 4 shows some results from the model and actual test data.

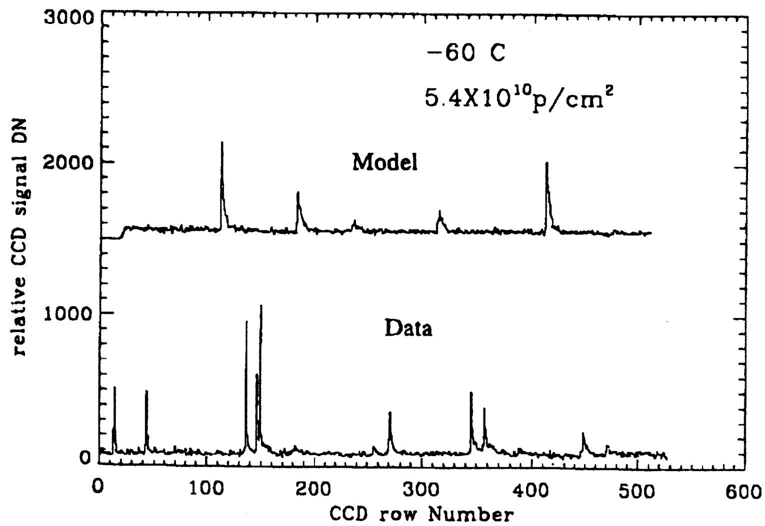

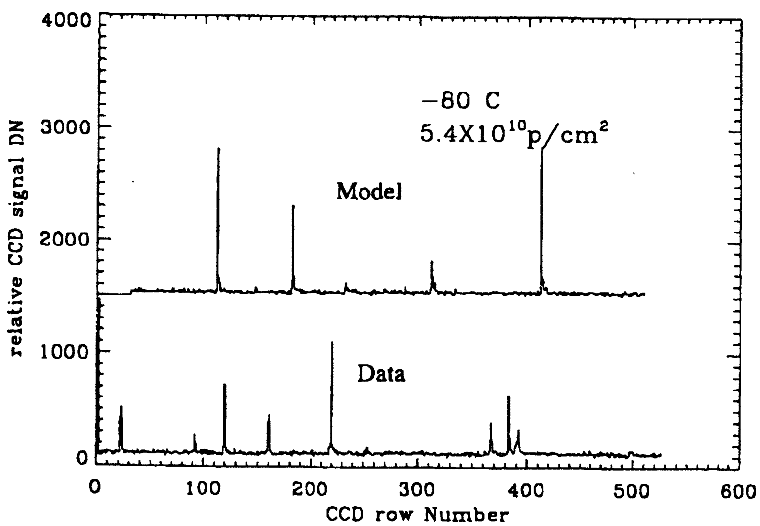

Figure 4: Simulated and actual data for a CCD illuminated by an Fe^{55} *source and at -60 and -80 C. The plots show a typical row in a 512X512 device. The model is the upper plot in each figure ant the data the lower.. The plots show a qualitatively reasonable agreement between the data and model.. To include for partial events the input data to the model had some pixel values that were less than 1620 electrons.*

6.0 Discussion

To test the robustness of the CTI model we predicted CTI "image smear" from a CCD with different operating parameters then those present here. Figure 5 shows a simulation of a CCD image where the transfer of a star image was modeled to determine the shift in the centroid due to radiation damage. The discrepancy between the centroid error calculated form the model image in figure 5 (lower plot) and that form actual data is about 25%.

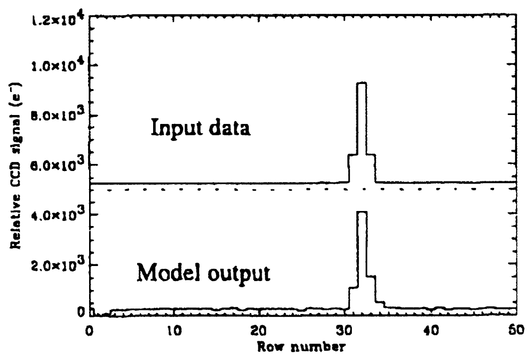

Figure 5: (upper plot) Input image. signal = 10,000 electrons total in a Guassian distribution with a DC dark current signal. Clocking rate is 166 MHz. CCD size 512X512 pixels (lower plot) Simulation of transferred image after CCD was irradiated with 63 MeV protons at a fluence of 5.4×10^{10} protons cm^{-2} . Predicted centroid error by CTI model is -0.17 pixel, actual centroid error measured from device modeled is -0.14 pixels

Further improvements of the model are currently being studied. For example, a more accurate calculation electric fields inside the bulk silicon can be made to better determine the actual size and shape of the electron cloud. To model CTI response at higher read rates (> 1 MHz) the trapping time constant of the traps could also be included.

7.0 References

A.M. Mohsen and M.F. Tompsett, "The Effects of Bulk Traps on the Performance of Bulk Channel Charge-Coupled Devices", IEEE Trans. El. Dev., Vol. ED-21, No. 11, pp. 701-712, Nov. 1974.

C. Dale, et al, IEEE Transactions On Nuclear Science, Vol. 40, NO. 6, pp. 1628-1636, Dec. 1993

A.D. Holland, Nuclear Instruments and Methods in Physics Research, A326 (1993), pp. 335-343

S.J. Watts, et al, IEEE Transactions On Nuclear Science, Vol. 43, NO. 6, pp. 2587-2594, Dec. 1996